VI International Conference on Computational Methods for Coupled Problems in Science and Engineering
COUPLED PROBLEMS 2015
B. Schrefler, E. Oñate and M. Papadrakakis (Eds)

PROPAGATION OF ACOUSTIC-GRAVITY WAVES IN INHOMOGENEOUS OCEAN ENVIRONMENT BASED ON MODAL EXPANSIONS AND HP-FEM

KOSTAS A. BELIBASSAKIS*, GERASSIMOS A. ATHANASSOULIS*, ANGELIKI E. KARPERAKI* AND THEODOSIOS K. PAPATHANASIOU†

* School of Naval Architecture and Marine Engineering
National Technical University of Athens
Heroon Polytechniou 9, Zografos 15773, Athens, Greece
e-mail: kbel@fluid.mech.ntua.gr, http://arion.naval.ntua.gr/~kbel/

† School of Applied Mathematical and Physical Science
National Technical University of Athens
Heroon Polytechniou 9, Zografos 15773, Athens, Greece
e-mail: papaththh@gmail.com

Key words: Acoustic-Gravity waves, Ocean Environment, Coupled-mode methods, FEM

Abstract. A coupled mode model is presented for the propagation of acoustic-gravity waves in layered ocean waveguides. The analysis extends previous work for acoustic waves in inhomogeneous environment. The coupled mode system is derived by means of a variational principle in conjunction with local mode series expansion, obtained by utilizing eigenfunction systems defined in the vertical section. These are obtained through the solution of vertical eigenvalue problems formulated along the waveguide. A crucial factor is the inclusion of additional modes accounting for the effects of spatialy varying boundaries and interfaces. This enhancement provides an implicit summation for the slowly convergent part of the local-mode series, rendering the series rapidly convergent, increasing substantialy the efficiency of the method. Particular aspects of the method include high order Lagrange Finite Element Methods for the solution of local vertical eigenvalue problems in the case of multilayered waveguides, and Gauss-type quadrature for the computation of the coupled-mode system coefficients. The above aspects make the present method quite efficient for long range propagation in extended waveguides, such as the ones found in geophysical applications, e.g. ocean basins, as only few modes are needed for the accurate representation of the wave field.

1 INTRODUCTION

Ocean waves generate acoustic modes in a wide range of acoustic frequencies, as a result of non-linear interactions of pairs of nearly opposing gravity waves having equal or nearly equal frequencies. In this case, the lower frequency part of the spectrum, nominally for frequencies lower than 2 Hz is caused by the nonlinearity of the hydrodynamic equations; see e.g., [1,2]. Also, in the low frequncy band, energetic acoustic–gravity waves appear as a result of seismic activity in the seabed and generation and propagation of tsunami waves; see, e.g., [3] and the references cited there. These waves propagating from the open sea to nearshore areas, interact

with various layers of the inhomogeneous ocean waveguide and the seabed, and are characterised by partial energy exchage of the modes, shoaling and scattering effects.

Wave propagation and scattering in an inhomogeneous waveguide is an interesting mathematical problem finding important applications, as, e.g., underwater acoustic propagation and scattering in shallow water and seismoacoustics [4, 5], atmospheric acoustics [6] and other. Several methods for treating this, generally non-separable, boundary value problem have been proposed, ranging from fully numerical, finite element and finite difference methods, to semi-analytical ones, like wavenumber integration, boundary integral equation and coupled-mode techniques, as well as various asymptotic models, like ray theory and the adiabatic and parabolic approximations; see e.g., [5, 7]. Fully numerical methods are computationally intense and thus, their use is more appropriate for short-range/low-frequency propagation and local scattering problems. In this work, a fast-convergent spectral model is presented for treating harmonic wave propagation and scattering problems in stratified, non uniform waveguides, governed by the Helmholtz equation. The method is based on a local mode series expansion, obtained by utilizing local eigenfunction systems defined through the solution of eigenvalue problems, formulated along the cross section of the waveguide. Following Belibassakis et al. [8] the local mode series are enhanced by including additional modes accounting for the effects of inhomogeneous waveguide boundaries and/or interfaces. The additional modes provide an implicit summation of the slowly convergent part of the local-mode series, rendering the remaining part to be fast convergent, increasing the efficiency of the method, especially in long-range propagation applications (see also [9] and [10]). Using the enhanced local mode expansion, in conjunction with an energy-type variational principle, a coupled-mode system of equations is derived for the determination of the unknown modal-amplitude functions. The numerical solution of the local vertical eigenvalue problems, in the case of multilayered waveguides, is obtained by means of *h*- and *p*-FEM (see, e.g., [8, 11]) exhibiting robustness and good rates of convergence. On the basis of the above, the coefficients of the coupled-mode system are calculated by numerical integration. Subsequently, the solution of the present coupled-mode system is obtained by using a finite difference scheme based on a uniform grid and using second-order central differences to approximate derivatives. Particular aspects of the method include high order Lagrange Finite Element Methods for the solution of local vertical eigenvalue problems in the case of multilayered waveguides, and Gauss-type quadrature for the computation of the coupled-mode system coefficients. The above aspects makes the present method quite efficient for long range propagation in extended waveguides, such as the ones found in geophysical applications, e.g. ocean basins, as only few modes are needed for the accurate representation of the unknown fields. Numerical examples are presented illustrating the efficiency of the present model, that can be naturally extended to treat propagation and scattering problems in more complicated 3D waveguides.

2 PROBLEM DESCRIPTION

Consider the multilayered waveguide of Fig.1. For simplicity we restrict ourselves to a 2D problem in an ocean acoustic environment, governed by Helmholtz equation. However, the present method and analysis can be naturally extended to more general 3D acoustic-gravity waveguides.

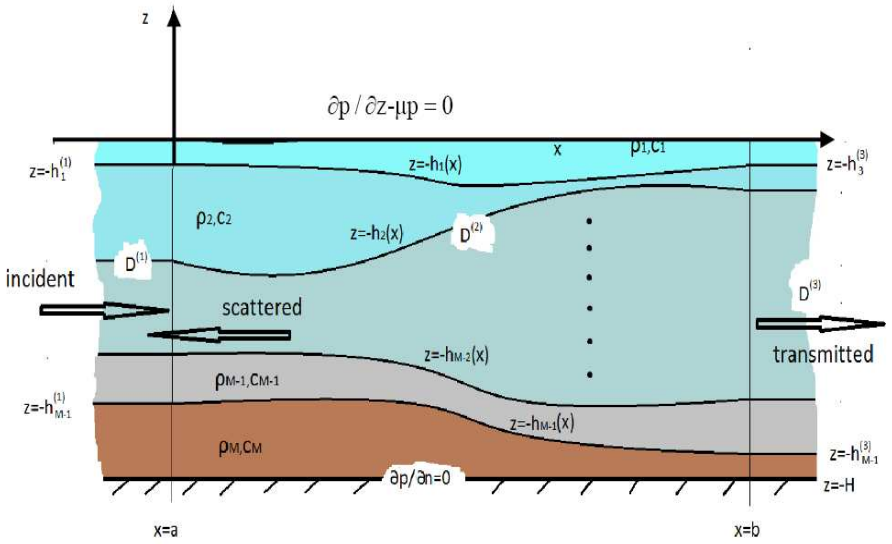

Figure 1: Multilayered two-dimensional acoustic waveguide.

The domain $D = D^{(1)} \bigcup D^{(2)} \bigcup D^{(3)}$ is decomposed into three parts $D^{(m)}$, $m = 1,2,3$ (see Fig. 1), as follows: $D^{(1)}$ is the subdomain characterized by $x_1 < a$ nand $D^{(3)}$ is the subdomain characterized by $x_1 > b$ $(b > a)$, and $D^{(2)}$ is the variable cross section subdomain lying between $D^{(1)}$ and $D^{(3)}$. A similar decomposition is also applied to the (upper and lower) boundaries, as well as to the internal interfaces.-The acoustic medium inside the domain is stratified. The physical properties of the layers, vary with respect to the (x,z) coordinates in the middle range-dependent subdomain $D^{(2)}$, and present only vertical variability in the two semi-infinite subdomains $D^{(1)}$ and $D^{(3)}$. Assuming that the whole domain consists of M layers, a total number of $M-1$ interfaces at $z = -h_j(x)$, $j = 1,2,...,M-1$, are considered, where $h_j(x)$ denotes the local depth of each interface (see Fig.1). The waveguide is terminated below by a perfectly rigid (acoustically hard) horizontal boundary, located at $z = -H$. On the other hand, the waveguide is terminated above by an acoustically soft boundary, located at $z = 0$, corresponding to the free surface.

The density ρ_j, $j = 1,2,..M$, of each layer is assumed to be constant within the layer, presenting possibly sharp discontinuities at the interfaces. Moreover, the sound speed $c_j(x,z)$, $j = 1,2,..M$, presents both vertical and horizontal variability in the middle subdomain $D^{(2)}$, and could also exhibit strong discontinuity at the interfaces. The sound speed becomes function only of z in the two semi-infinite subdomains $D^{(1)}$ and $D^{(3)}$, which are then range independent subdomains with respect to both geometry and physical parameters. This fact permits us to obtain complete expansions of the wave field in the above semi-infinite regions by means of separation of variables, and consistently formulate the conditions of wave incidence and transmission at $x=a$ and $x=b$, respectively.

2.1 Governing Equations

Restricting ourselves to monochromatic waves of angular frequency $\omega=2\pi f$, the acoustic harmonic wave propagation problem inside the present multi-layered waveguide is governed by the Helmholtz equation. The respective boundary value problem takes the form of finding the continuous function p representing the acoustic pressure such that

$$\nabla\cdot\left(\frac{1}{\rho}\nabla p\right)+\frac{k^2}{\rho}p=0\ ,\ \text{in}\quad D \tag{1}$$

where the wavenumber $k(x,z)=\omega/c(x,z)$ is a piecewise smooth function of the spatial coordinates, possibly presenting sharp discontinuities at the interfaces $z=-h_j(x),\quad j=1,2,...,M-1$. Eq. (1) is supplemented by the following boundary conditions

$$\partial p/\partial z-\mu p=0\,,\quad \text{on the free surface}\quad z=0\,, \tag{2}$$

$$\partial p/\partial n=\partial p/\partial z=0\,,\ \text{on the perfectly rigid (terminating) boundary at}\ \ z=-H\,, \tag{3}$$

where $\mu=\omega^2/g$ is the frequency parameter of gravity waves (g=9.81m/s^2), in conjunction with the interface conditions

$$\frac{1}{\rho_j}\frac{\partial p}{\partial n}=\frac{1}{\rho_{j+1}}\frac{\partial p}{\partial n}\quad\text{on}\quad z=-h_j(x),\quad j=1,2,...,M-1\,. \tag{4}$$

In the previous equations $\partial p/\partial n=\mathbf{n}\nabla p$ denotes the normal derivative, where $\mathbf{n}$ is the unit normal vector on each boundary and interface. We consider a transmission problem forced by plane waves propagating in the positive x direction. The waves are incident from $D^{(1)}$, and then they are refracted and scattered in the range dependent subdomain $D^{(2)}$, and finally transmitted in $D^{(3)}$. In order to treat the present problem in the infinite domain, complete normal-mode type representations of the wave field in the regions of incidence $D^{(1)}$ and transmission $D^{(3)}$ are derived by separation of variables. In particular, the expansion of the wavefield in $D^{(1)}$ consists of incident and reflected (scattered) waves is as follows,

$$p^{(1)}=\sum_{n=1}^{\infty}\left(A_n^{(1)}e^{ik_n^{(1)}x}+B_n^{(1)}e^{-ik_n^{(1)}x}\right)Z_n^{(1)}(z) \tag{5}$$

where the functions $Z_n^{(1)}(z)$ and the numbers $k_n^{(1)},\ n=1,2,3...,$ satisfy the following vertical eigenvalue problem in $D^{(1)}$

$$\frac{d^2Z_n^{(1)}}{dz^2}+\left[\left(k^{(1)}(z)\right)^2-(k_n^{(1)})^2\right]Z_n^{(1)}=0\,, \tag{6}$$

$$\frac{dZ_n^{(1)}(z=0)}{dz}-\mu Z_n^{(1)}(z=0)=0,\qquad \frac{dZ_n^{(1)}(z=-H)}{dz}=0\,, \tag{7a,b}$$

in conjunction with the interface condition,

$$Z_n^{(1)}(-h_j^{(1)}+0) = Z_n^{(1)}(-h_j^{(1)}-0), \quad j=1,2,\, M-1\,, \tag{8}$$

$$\frac{1}{\rho_j}\frac{\partial Z_n^{(1)}(-h_j^{(1)}+0)}{\partial z} = \frac{1}{\rho_{j+1}}\frac{Z_n^{(1)}(-h_j^{(1)}-0)}{\partial z}, \quad j=1,2,\, M-1\,, \tag{9}$$

where $k^{(1)}(z)=\omega/c^{(1)}(z)$. Similarly, the expansion of the acoustic wavefield in the region of transmission $D^{(3)}$, consists only of outgoing radiated waves, and is given by

$$p^{(3)} = \sum_{n=1}^{\infty}\left(A_n^{(3)}e^{ik_n^{(1)}x}\right)Z_n^{(3)}(z)\,, \tag{10}$$

where the eigenfunctions $Z_n^{(3)}(z)$ and the corresponding eigenvalues $k_n^{(3)}$, $n=1,2,3...$, are obtained by similar as above vertical eigenvalue problems formulated in $D^{(3)}$. From the properties of regular Sturm-Liouville problems ([12], [13]) the eigenvalues $\left\{\left(k_n^{(m)}\right)^2, n=1,2..\right\}$, m=1,3, are discrete, infinite, with continuously decreasing moduli, and thus, the corresponding parameters $\left\{k_n^{(m)},\, n=1,2,3...\right\}$, are subdivided into a finite real subset $\left\{k_n^{(m)},\, n=1,2,3...N_p^{(m)}\right\}$ and an infinite imaginary one $\left\{i\left|k_n^{(m)}\right|,\, n=N_p^{(m)}+1,....\right\}$, where $N_p^{(m)}$, denotes the number of propagating modes in $D^{(m)}$, $m=1,3$. The first eigenvalue (n=1) and corresponding eigenvector is essentially associated with the free-surface gravity mode which presents fast decay in depth.

Clearly, in order for the wave field to remain bounded at infinity, the coefficients of the expansion $A_n^{(1)}=0,\, n>N_p^{(1)}$. On the other hand the terms $A_n^{(1)}\exp\left(ik_n^{(1)}x\right)Z_n^{(1)}(z)$, $n\le N_p^{(1)}$, constitute the given data associated the incident wave field. Due to the linearity of the problem each one of the above terms could be separately considered as forcing of the present acoustic waveguide and the solutions is obtained by superposition of the responses. In addition, the terms $\exp\left(-ik_n^{(1)}x\right)Z_n^{(1)}(z)$, $n>N_p^{(1)}$, and $\exp\left(ik_n^{(3)}x\right)Z_n^{(3)}(z)$, $n>N_p^{(3)}$, are the evanescent modes in $D^{(m)}$, $m=1,3$, respectively. These modes decay exponentially at large distances from the inhomogeneity in the two semi-infinite strips. By exploiting the representations (5) and (10), the problem can be formulated as a transmission boundary value problem in the bounded subdomain $D^{(2)}$, satisfying Eq. (1), (2) (3) and (4) and the following matching conditions:

$$p^{(2)}(x,z)=p^{(1)}(x,z), \qquad \frac{\partial p^{(2)}}{\partial x^{(2)}}=\frac{\partial p^{(1)}}{\partial x^{(1)}}\,, \quad x=a\,, \quad -H<z<0, \tag{11a}$$

$$p^{(2)}(x,z)=p^{(3)}(x,z), \qquad \frac{\partial p^{(2)}}{\partial x}=\frac{\partial p^{(3)}}{\partial x}\,, \quad x_1=b, \quad -H<z<0\,. \tag{11b}$$

2.2 Variational Formulation

We proceed to formulate a functional $\mathscr{F}$ allowing us to state a variational formulation of the transmission problem. The admissible function space for the wave field $p^{(2)}(x,z) \in D^{(2)}$ (simply denoted from now on as p), consists of globally continuous and piecewise smooth functions, possessing continuous second derivatives in the interior of each layer, such that

$$\frac{\partial p(x,z=0)}{\partial z} - \mu p(x,z=0) = 0 \tag{12}$$

For this purpose, we consider the following energy-type functional

$$\begin{aligned} \mathscr{F}\left(p\ ,\left\{B_n^{(1)}\right\},\left\{A_n^{(3)}\right\}\right) = \ & \frac{1}{2}\int_{D^{(2)}}\left[\rho^{-1}\left(\nabla p\ \right)^2 - \rho^{-1}k^2\left(p\ \right)^2\right]dxdz + \frac{1}{2\rho_1}\int_{x=a}^{x=b}\mu p^2 dx + \\ -\int_{z=-H}^{z=\eta_3}\left(p - \frac{1}{2}p^{(3)}\left(\left\{A_n^{(3)}\right\}\right)\right)\frac{\partial p^{(3)}\left(\left\{A_n^{(3)}\right\}\right)}{\partial x}dz \ & + \int_{z=-H}^{z=\eta_1}\left(p - \frac{1}{2}p^{(1)}\left(\left\{B_n^{(1)}\right\}\right)\right)\frac{\partial p^{(1)}\left(\left\{B_n^{(1)}\right\}\right)}{\partial x}dz\ . \end{aligned} \tag{13}$$

The present problem admits of an equivalent variational formulation expressed by

$$\delta\mathscr{F}\left(p\ ;\left\{B_n^{(1)}\right\},\left\{A_n^{(3)}\right\}\right) = 0 \tag{14}$$

Using Green's theorem in conjunction with Eq. (12), the above variational equation takes the form

$$\begin{aligned} & -\int_{D^{(2)}}\left(\nabla\cdot\left(\rho^{-1}\nabla p\right)+\rho^{-1}k^2 p\right)\delta p\ \ dxdz + \int_{z=-H}^{z=\eta_1}\left(p\ - p^{(1)}\right)\ \delta\frac{\partial p^{(1)}}{\partial x}dz\ + \\ & -\int_{z=-H}^{z=\eta_3}\left(p\ - p^{(3)}\right)\delta\frac{\partial p^{(3)}}{\partial x}dz - \int_{z=-H}^{z=\eta_1}\left(\frac{\partial p}{\partial x} - \frac{\partial p^{(1)}}{\partial x}\right)\delta p\ dz\ + \\ & -\int_{z=-H}^{z=\eta_3}\left(\frac{\partial p}{\partial x} - \frac{\partial p^{(3)}}{\partial x}\right)\delta p\ \ dz\ - \sum_{j=1}^{M-1}\int_{z=-h_j(x)}\left(\frac{1}{\rho_j}\frac{\partial p}{\partial N} - \frac{1}{\rho_{j+1}}\frac{\partial p}{\partial N}\right)\delta p\, dx = \ 0\,, \end{aligned} \tag{15}$$

where $\left.\frac{\partial p}{\partial N}\right|_{z=-h_j(x)} = \frac{\partial p}{\partial z} + \frac{dh_j}{dx}\frac{\partial p}{\partial x}$. The usefulness of the above variational principle hinges on the fact that it leaves us the freedom to choose any particular representation for the unknown field $p(x,z) \in D^{(2)}$. In this way, a variety of possible algorithms for the numerical solution of the present wave problem can be constructed.

3 ENHANCED LOCAL MODE REPRESENTATION

Inside the bounded domain $D^{(2)}$, the solution $p(x,z)$ may be set into a standard spectral-type representation, based on local-mode series, as follows

$$p\ (x,z)=\sum_{n=1}^{\infty}U_n(x)Z_n(z;x)\,. \tag{16}$$

The family of local vertical basis functions $Z_n(z;x)$ appearing in the above expansion, which are parametrically dependent on x, is obtained by formulating and solving local, vertical Sturm-Liouville problems in the z-intervals $[-H,\,0]$, for each horizontal position $a<x<b$. However, any finite truncation of the series (16) is incompatible with any of the sloping interface conditions, whenever $dh_j(x)/dx\neq 0$, $j=1,2,...M-1$, rendering the above series to converge only in an L^2-sense, and the coefficients U_n to decay like $O\left(n^{-2}\right)$; see Belibassakis et al [8]. To remedy this inconsistency, an additional mode associated with each interface is introduced, denoted by $U_j(x)Z_j(z;x)$, $j=-M+2,..,-1,0$. These modes are called sloping-interface modes. Thus, we obtain the following enhanced local-mode series

$$p(x,z)=\sum_{n=-M+2}^{0}U_n(x)Z_n(z;x)+\sum_{n=1}^{\infty}U_n(x)Z_n(z;x)\,. \tag{17}$$

The vertical structure of the sloping-interface modes, for every horizontal position $a<x<b$, is any globally continuous and piecewise smooth function defined with support in the local vertical intervals $[-h_{M-1}(x),-h_{M-2}(x)],....,[-h_1(x),0]$, satisfying the following condition(s)

$$\left.\frac{1}{\rho_j}\frac{\partial Z_n}{\partial z}\right|_{z=-h_j}-\left.\frac{1}{\rho_{j+1}}\frac{\partial Z_n}{\partial z}\right|_{z=-h_j}=1,\quad j=1,2,...,M-1\,. \tag{18}$$

Moreover, the function $Z_0(z;x)$ should satisfy the homogeneous Dirichlet condition at $z=\eta(x)$. Consequently, the M-1 terms $U_j(x)Z_j(z;x)$, $j=-M+2,..,-1,0$, are additional degrees of freedom in the bounded subdomain $D^{(2)}$, permitting the consistent satisfaction of all interface conditions. The amplitude of the additional modes is given by

$$U_{j-1}(x)=\left.\frac{1}{\rho_j}\frac{\partial p}{\partial z}\right|_{z=-h_j}-\left.\frac{1}{\rho_{j+1}}\frac{\partial p}{\partial z}\right|_{z=-h_j},\quad j=1,2,..M-1\,. \tag{19}$$

From this last relation, it is evident that no extra mode needs to be introduced in the last layer terminated in the lower flat boundary, where a homogeneous Neumann condition is satisfied.

The important effect of the additional modes is to significantly increase the rate of decay of Z_n – Fourier coefficients of the acoustic wave potential (modal amplitudes). In this case, the modes associated with the enhanced series exhibit a rapid decay rate: $\left|U_n(x)\right|\le C(x)\,n^{-4}$, $n\to\infty$, $\forall x\in[a,b]$. The bound $C(x)$ is a continuous function on $[a,b]$ and, thus, the previous estimate is global: ; see also [9,10]. If the additional modes are not included, then the

rate of decay of the modes in the standard series (16) is only $|U_n| = O\left(n^{-2}\right)$. The above result is obtained by means of repetitive use of integration by parts, in conjunction with the properties of the local Sturm-Liouville system, and will be illustrated through appropriate numerical examples in a subsequent section.

4 FEM SOLUTION OF THE LOCAL VEP

In this section we will describe the finite element method, as applied to the solution of the vertical eigenvalue problem (vep). In the following we adopt the notation by Hughes [11]. We assume that for all x in the interval $a<x<b$, it is $\rho(z;x)$, $k^2(z;x) \in L^\infty(-H,0)$.

Let us introduce the (Sobolev) function spaces $H^1_{|E(x)} \triangleq \left\{u : u \in H^1(-H,0),\ \mathrm{x} \in [\mathrm{a,b}]\right\}$. The continuous vertical eigenvalue problem, at each horizontal position, can now be stated in variational form as follows

$$\text{Find } (\lambda, p) \in \mathbb{R} \times H^1_{0|E(x)} \text{ such that } a(w,p) = \lambda b(w,p)\ ,\ \forall w \in H^1_{|E(x)}\,, \tag{20}$$

Where

$$a(w,p) = \int_{-H}^{0} \rho^{-1} \frac{dw}{dz}\frac{dp}{dz} dz - \int_{-H}^{0} k^2 \rho^{-1} wp dz + \rho^{-1}\mu\left[wp\right]_{z=0}\,, \tag{21a}$$

$$b(w,u) = -\int_{-H}^{0} \rho^{-1} wp dz\,, \tag{21b}$$

Assume a partition of $[-H,0]$, of the form $-H = z_1 < z_2 < ..... < z_{N+1} = 0$, with $N \in \mathbb{N}$ and $N > M$ (M being the number of layers in the waveguide). The partition is such that $\forall x$ the interface positions coincide with $M-1$ nodes. We introduce the sequence of finite element sub-spaces,

$$V^h \triangleq \left\{u^h \in H^1(-H,0) : u^h\Big|_{[z_i, z_{i+1}]} \equiv \mathrm{P}_\ell(\mathrm{z}),\ \ i = 1,2,...,N,\ \ell \in \mathbb{N},\ \mathrm{x} \in [\mathrm{a,b}]\right\}$$

where $P_\ell(z)$ is a polynomial of degree ℓ. Obviously $V^h \subset H^1_{|E(x)}$. The discrete variational formulation of the vertival eigenvalue problem takes the following form:

$$\text{Find } (\lambda^h, p^h) \in \mathbb{R} \times V^h \text{ such that } a(w^h, p^h) = \lambda^h b(w^h, p^h)\ ,\ \forall w^h \in V^h \tag{22}$$

In the following analysis we assume piecewise linear, quadratic and cubic interpolations for the finite element solution, i.e. $\ell = 1, 2 \text{ and } 3$. Regardless of the interpolation degree, the desired solution has the form,

$$p^h = \sum_{j=1}^{N} c_j N_j(z)\,. \tag{23}$$

where $N_j \in V^h$. Introducing the above expansion in Eq. (22), the discrete variational formulation finally becomes an eigenvalue matrix equation of the form:

$$\mathbf{A}\,\mathbf{u} = \lambda\,\mathbf{B}\,\mathbf{u}\ , \tag{24}$$

where the elements of the $N \times N$ matrices $\mathbf{A}$ and $\mathbf{B}$ are $a_{ij} = a(N_i, N_j)$ and $b_{ij} = b(N_i, N_j)$, $i, j = 1,2,..,N$, respectively.

4.1 Numerical solution of VEP

As demonstrative examples we consider the case of an acoustic environment of total thickness (depth) $H = 1000m$, consisting of two layers of thickness 100m (upper) and 900m (lower) and equal thickness 500m, respectively. In the first case the position of the internal interface is at a depth $h_1 = 100m$, and in the second at $h_1 = 500m$. Moreover, two frequencies have been considered $f = 2Hz$ and $f = 0.08Hz$. Both the density and speed of sound are assumed to be constant within each layer. For the upper layer corresponding to water these quantities are $\rho_1 = 1g/cm^3$, $c_1 = 1500m/\sec$, and for the lower layer $\rho_2 = 1.5g/cm^3$, $c_2 = 1700\ m/\mathrm{s}$, corresponding to sediment. Details concerning the exact analytical solution of this problem are included in the APPENDIX 1.

The first 5 eigenfunctions for *f*=2Hz are shown in Fig. 2. A zoom on the upper 10m is shown in the right subplot, illustrating the layered structure of the free-surface (gravity) mode (*n*=1), which presents exponetial decay in depth. Corresponding resuts for the lower frequency *f*=0.08Hz are plotted in Fig.3, for two positions of the interface at 100m (left subplot) and 500m (right subplot), which is indicated by using thick dashed lines. In the above plots the first eigenfunction (*n*=1) associated with the free-surface (gravity) mode is normalizad with its maximum value at z=0, while the rest of the modes (*n*=2,3,4…) are normalizad with respect to their values at the bottom (*z*=-*H*). With increasing frequency parameter μ, a positive sway of the first eigenvalue, is observed leading to the formation of a boundary layer visible in the sublot of Fig. 2. The eigenvalues as computed with the finite element method, using $N = 20, 40, 80$ elements, are in perfect match when compared against the exact solution for the first modes.A series of numerical results are shown for the case of placing the interface at $h_1 = 100m$ and $f = 0.08Hz$. In Fig. 4 a comparison between the first exact and computed eigenvalues is shown for different number of elements, $N = 20, 40 \text{ and } 80$, and two different interpolation degrees, $p = 1 \text{ and } 2$. It is observed that the error of the numerical solution for the eigenvalues is found to increase with increasing eigenvalue numbers. The convergence of the finite element solution for the 5th, 10th and 15th eigenvalues is demonstrated in Fig. 5. Convergence rates are observed for increasing interpolation degree, $p = 1, 2 \text{ and } 3$ and are found to be 2, 4 and 6 respectively. Enhanced rates have been obtained by raising the degree ℓ of the piecewise polynomials.

5 THE COUPLED - MODE SYSTEM

Having obtained the eigenfunctions associated with the local vertical problem, $\forall x \in [a,b]$, we proceed to the calculation of the mode amplitudes $\{U_j(x),\ \ j = -M+2,..,-1,0,1,2,.....\}$. To this respect we substitute the enhanced local mode representation (17) in the variational

principle (15), and express the variation of the unknown field $p(x,z) \in D^{(2)}$, through the variations of the modal amplitudes

$$\delta p(x,z) = \sum_{n=-M+1}^{\infty} Z_n(z;x)\, \delta U_n(x) \quad . \tag{25}$$

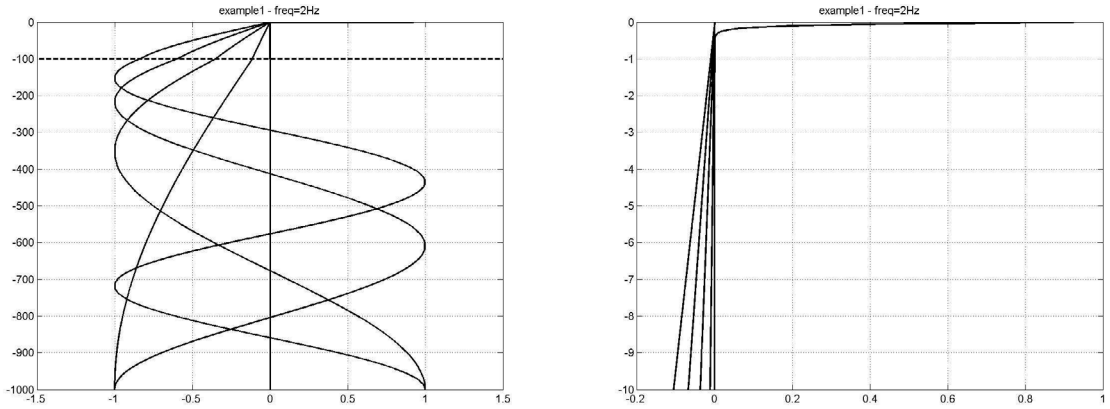

Figure 2: First 5 eigenfunctions for *f*=0.2Hz. The position of the interface is at 100m is indicated in the left subplot by thick dashed lines. A zoom on the upper 10m is shown in the right subplot, illustrating the layered structure of the free-surface (gravity) mode (*n*=1).

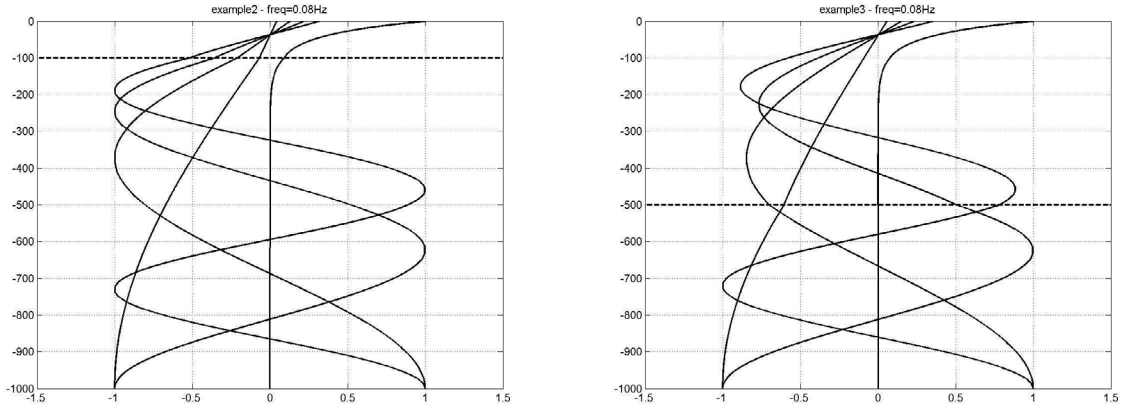

Figure 3: First 5 eigenfunctions in the low frequency case *f*=0.08Hz. The position of the interface at 100m (left subplot) and 500m (right subplot) is indicated by thick dashed lines.

Next, by considering only the variations $\delta U_n(x),\ n = -M+2,..,0,1,...$, in $a < x < b$, we obtain from the first term in the left hand side of Eq. (16) the following coupled-mode system (CMS) of second-order ordinary differential equations, with respect to the mode amplitudes, $U_n(x), n = -M+2,..,0,1,2,..$,

$$\sum_{n=-M+2}^{\infty} a_{mn}(x)\frac{d^2U_n(x)}{dx^2} + b_{mn}(x)\frac{dU_n(x)}{dx} + c_{mn}(x)U_n(x) = 0\,, \tag{26}$$

where $m = -M+2,..,0,1,2,...$ The x-dependent coefficients a_{mn}, b_{mn} and c_{mn} are defined in terms of $Z_n(z;x)$ in $a < x < b$ and are given by

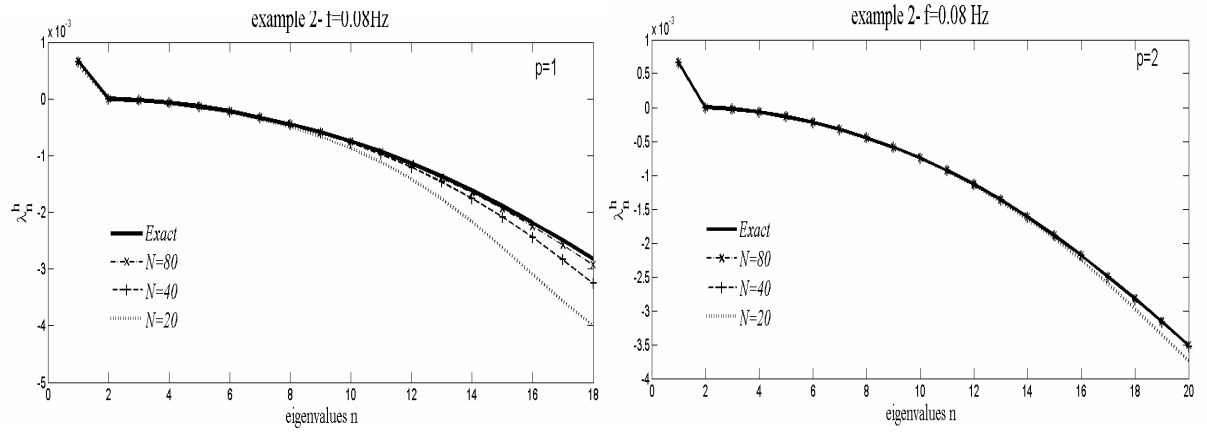

Figure 4: Comparison between the computed eigenvalues against the exact solution (thick line) for $p=1$ (left) and $p=2$ (right).

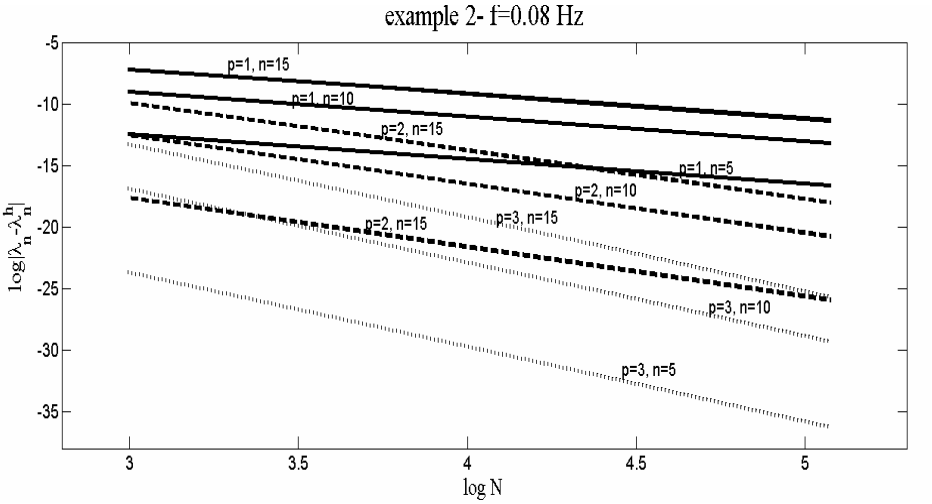

Figure 5: Convergence of the finite element solution for the 5th, 10th and 15th eigenvalues, using $p=1,2$ and 3.

$$a_{mn} = \langle Z_n, Z_m \rangle, \tag{27}$$

$$b_{mn} = 2\left\langle \frac{\partial Z_n}{\partial x}, Z_m \right\rangle + \sum_{j=1}^{M-1} \left(\frac{1}{\rho_j} - \frac{1}{\rho_{j+1}} \right) \frac{dh_j}{dx} Z_n(-h_j) Z_m(-h_j), \tag{28}$$

$$c_{mn} = \left\langle \frac{\partial^2 Z_n}{\partial x^2} + \frac{\partial^2 Z_n}{\partial z^2} + k^2 Z_n, Z_m \right\rangle + \sum_{j=1}^{M-1} \left([\![Z_{n,z}]\!] + \frac{dh_j}{dx} [\![Z_{n,x}]\!] \right) Z_m(-h_j). \tag{29}$$

In the above relations, $\langle f,g\rangle := \int_{-H}^{\eta} \rho^{-1} f(z)g(z)dz$ is the weighted inner product of $L^2(-H,0)$ function spaces, for all x in $a < x < b$. Further, the quantities $[\![Z_n]\!]_x$ are defined by

$$[\![Z_{n,w}]\!] = \left[\frac{1}{\rho_j} \frac{\partial Z_n}{\partial w}\bigg|_{z=-h_j^+} - \frac{1}{\rho_{j+1}} \frac{\partial Z_n}{\partial w}\bigg|_{z=-h_j^-} \right], \; j = 1,2,...,M-1 . \tag{30}$$

From the last four terms in the left-hand side of the variational equation (16), defined on the vertical interfaces at $x = a$ and $x = b$, respectively, we obtain the following end-conditions for the mode amplitudes $U_n(x)$,

$$C_n^{(m)} dU_n / dx_1 + D_n^{(m)} U_n = F_n^{(m)}, \quad n = 0,1,2,..., m = 1,3, \tag{31}$$

where the coefficients $C_n^{(m)}, D_n^{(m)}, F_n^{(m)}$, $m = 1,3$, are defined in terms of the physical parameters at the end points $x = a$ and $x = b$.

6 NUMERICAL RESULTS AND DISCUSSION

In the present work, the numerical solution of the above coupled-mode system is obtained by truncating the series (17) and using a finite difference scheme based on a uniform grid and second-order central differences to approximate derivatives. In order to further enhance the efficiency of the present model, future work is focused on the application of *p*-Finite Element Methods, in conjunction with grid adaptation techniques based on the spatial variability of the system coefficients a_{mn}, b_{mn} and c_{mn}.

As an example, we consider underwater acoustic propagation in a coastal environment, characterized by variable seabed boundary. As before, the upper layer (layer 1) is sea water of density and speed of sound $\rho_1 = 1g/cm^3$, $c_1 = 1500\,m/\mathrm{s}$. The lower layer (layer 2) corresponds to sand-silt-clay sediment with properties $\rho_2 = 1.5g/cm^3$, $c_2 = 1700\ m/\mathrm{s}$, terminated at the impermeable (rigid) bottom which is located at a depth $z = -100m$. The geometry of the internal interface is defined as

$$h_1(x) = 500 - 450 \tanh\left[2\pi \left(\left(\frac{x-3000}{4000} \right) - 0.5 \right) \right], \quad a \le x \le b \quad , \tag{32}$$

where *a*=2800m and *b*=7200m.

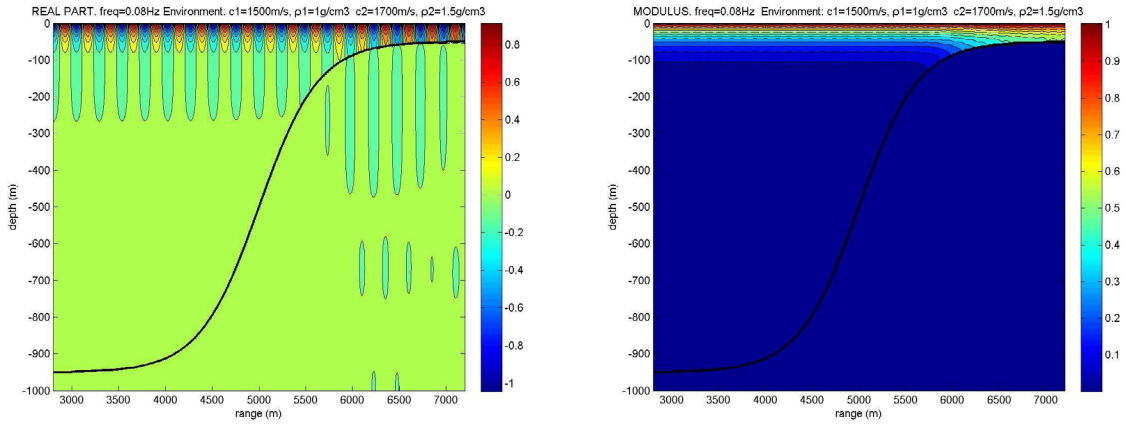

Figure 6: Acoustic pressure (real part). Frequency 0.08 Hz. Excitation by the first surface (gravity) mode, *n*=1. Parameters: $\rho_1 = 1g/cm^3, c_1 = 1500m/\mathrm{s}$, $\rho_2 = 1.5g/cm^3, c_2 = 1700m/\mathrm{s}$.

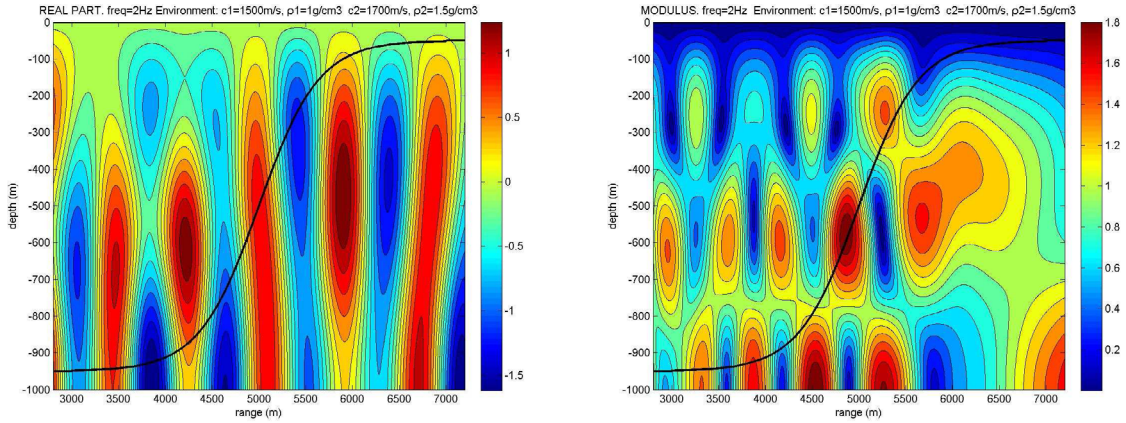

Figure 7: Acoustic pressure (modulus). Frequency 2 Hz. Excitation by the second interior (acoustic) mode *n*=2, and acoustic parameters same as in Fig.6.

Numerical results concerning the real part of the calculated wave field and its modulus, forced by the first incident mode *n*=1, when the waveguide is excited at frequency $f = 0.08Hz$ and by the second incident mode *n*=2, for $f = 2Hz$ are shown in Fig. 6 and 7, respectively, as obtained by present method. In the case of Fig.4 there is only one propagating mode (*n*=1), while in Fig.7 the number of propagating modes is 3 (*n*=1,2,3) both in the regions of incidence and transmission. The local-mode series is truncated by keeping 5 totally modes, and the coupled-mode system is discretized using 1200 segments, which were proved to be enough for numerical convergence. It can be seen that in the low frequency case $f = 0.08Hz$ the gravity mode interacts very little with the rest of the modes. Near the shallow end of the domain small part of the energy is transmitted from the upper medium (water) to the lower medium (sediment). Also, in the case of higher frequency $f = 2Hz$ the interaction of the first acoustic mode (*n*=2) with the gravity mode (*n*=1) is very small and the generated free-surface elevation is negligible. Thus, the acoustic mode is difficult to be observed at the free surface, however this could become possible at lower depths under the free surface.

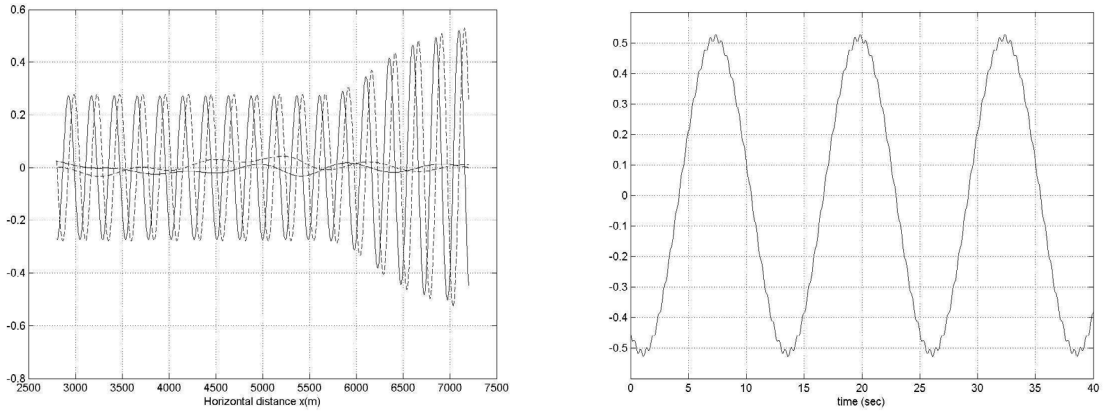

Figure 8: (a) Pressure at depth 50m for frequency f=0.08Hz with excitation by the free surface (gravity) mode n=1 of unit amplitude, and for f=2 Hz with excitation by the second interior (acoustic) mode n=2 of 10 times smaller amplitude. (b) Pressure signal at depth 50m at the shallow end of the domain b=7200m.

As an example we present in Fig.6 the pressure distribution at depth 50m (location of the seabed in the shallow end of the domain) calculated for frequency f=0.08Hz with excitation by the free surface (gravity) mode n=1 of unit amplitude, and for f=2 Hz with excitation by the second (acoustic) mode n=2 of 10 times smaller amplitude, which is in compatibility with the spectrum characteristics of tsunami waves generated by bottom dislocation. For this example the pressure signal at depth 50m at the shallow end of the domain is plotted in the right subplot of Fig.8, where the acoustic-gravity waves associated with the mode n=2 are clearly observable as high frequency ripples. The latter travel at significant higher speed that the free surface waves associated with the first mode at f=0.08Hz leaving an option for an advance warning sufficient for evacuation and protection.

7 CONCLUSIONS

In this work an improved coupled-mode method is presented for the efficient solution of the problem of time-harmonic propagation and scattering of acoustic-gravity waves in a non uniform stratified waveguide. The problem is governed by the Helmholtz equation, with variable coefficients, in conjunction with the linearized free-surface boundary condition associated with gravity waves. Our method is based on an enhanced local-mode series for the representation of the wave field, including additional modes, accounting for the effects of the inhomogeneous interfaces. In the case of multilayered waveguides, the local vertical eigenvalue problems are treated by h- and p-FEM, exhibiting robustness and good rates of convergence. In order to further enhance the efficiency of the present model, current work is focused on the application of hp-FEM for the solution of the coupled systen on thehorizontal plane, in conjunction with grid adaptation techniques based on the spatial variability of the system coefficients. Among several other advantages, the present method can be naturally extended to treat wave propagation and scattering problems in 3D multi-layered waveguides.

REFERENCES

[1] Ardhuin, F. Stutzmann E., Schimmel, M. and Mangeney A. Ocean wave sources of seismic noise. *J. Geophys. Res.*, (2011) **116**: C09004, doi:10.1029/2011JC006952.

[2] Ardhuin F., and Herbers, T.H.C. Noise generation in the solid Earth, oceans and atmosphere, from nonlinear interacting surface gravity waves in finite depth. *J. Fluid Mech.* (2013) **716**:316–348.

[3] Stiassnie, M. Tsunamis and acoustic-gravity waves from underwater Earthquakes. *J. Eng Math* (2010) **67**:23–32, doi: 10.1007/s10665-009-9323-x.

[4] Boyles, C.A. *Acoustic waveguides. Applications to ocean science*. J.Wiley & Sons, (1984).

[5] Jensen, F., Kupperman, W., Porter, M. and Schmidt, H. *Computational Ocean Acoustics*, AIP Press, (1994).

[6] Salomons, E.M. *Computational Atmospheric Acoustics*, Kluwer Academic Publishers, Dordrecht (2001).

[7] Lee, D. and Schultz, M.H. *Numerical Ocean Acoustic Propagation in Three Dimensions*, World Scientific, Singapore (1995).

[8] Belibassakis, K.A., Athanassoulis, G.A, Papathanasiou, T.K., Filopoulos, S.P. and Markolefas S. Acoustic wave propagation in inhomogeneous, layered waveguides based on modal expansions and hp-FEM. *Wave Motion* (2014) **51**:1021–1043.

[9] Athanassoulis, G.A and Belibassakis, K.A. A consistent coupled-mode theory for the propagation of small-amplitude water waves over variable bathymetry regions. *J. Fluid Mech.* (1999) **389**: 275-301.

[10] Athanassoulis, G.A., Belibassakis, K.A., Mitsoudis, D.A., Kampanis, N.A. and Dougalis, V.A. Coupled-mode and finite-element solutions of underwater sound propagation problems in stratified acoustic environments. *J. Comput. Acoust.* (2008) **16**(1): 83-116.

[11] Hughes, T.J.R. *The Finite Element Method, Linear Static and Dynamic Finite Element Analysis,* Dover Publications INC, (1987).

[12] Coddington, E. and Levinson, N. *Theory of Ordinary Differential Equations*, McGraw Hill, (1955).

[13] Tichmarsh, E.G. *Eigenfunction expansions*, Calderon Press, (1962).

APPENDIX

In the case of two layers $1,2$, with constant physical properties $\rho_1, c_1, k_1 = \omega/c_1$ and $\rho_2, c_2, k_2 = \omega/c_2$ respectively, the exact analytical solution of the vertical eigenvalue problem is given by

$$Z_{(1)}(z) = B_n\left[b_n \cos(\lambda_{n1} z) + \sin(\lambda_{n1} z)\right] \quad , \qquad Z_{(2)}(z) = B_n K_n \cos\left[\lambda_{n2}(z+H)\right] \quad , \qquad \text{(A1)}$$

where

$$\lambda_{n1} = \sqrt{k_1^{\,2} - k_n^{\,2}} \quad , \qquad \lambda_{n2} = \sqrt{k_2^{\,2} - k_n^{\,2}} \quad , \tag{A2}$$

and

$$b_n = \frac{\lambda_{n1}}{\mu} , \qquad K_n = \frac{b_n \cos(-\lambda_{n1} h_1) + \sin(-\lambda_{n1} h_1)}{\cos\left(\lambda_{n2} h_2\right)} . \tag{A3}$$

In this case, the eigenvalues k_n are found as the roots of the equation

$$\frac{\rho_2 \lambda_{n1}}{\rho_1 \lambda_{n2}} \left[b_n \sin(\lambda_{n1} h_1) + \cos(-\lambda_{n1} h_1) \right] = \tan(\lambda_{n2} h_2) \left[\sin(\lambda_{n1} h_1) - b_n \cos(-\lambda_{n1} h_1) \right], \tag{A4}$$

which expresses the continuity of $\rho^{-1} \partial Z / \partial z$ across the interface at $z = -h_1$. The remaining constants B_n, $n = 1, 2, \ldots.$, of the above solution can be fixed by appropriate normalization.